Differential Patterns of MicroRNA Expression in Neuroblastoma Are Correlated with Prognosis, Differentiation, and Apoptosis

Yongxin Chen and Raymond L. Stallings

Children's Cancer Research Institute and Department of Pediatrics, The University of Texas Health Science Center at San Antonio, San Antonio, Texas

Abstract

Neuroblastoma accounts for 15% of pediatric cancer deaths, and although a few protein-coding genes, such as *MYCN*, are involved with aggressive pathogenicity, the identification of novel biological targets for therapeutic intervention is still a necessary prerequisite for improving patient survival. Expression profiling of 157 microRNA (miRNA) loci in 35 primary neuroblastoma tumors indicates that 32 loci are differentially expressed in favorable and unfavorable tumor subtypes, indicating a potential role of miRNAs in neuroblastoma pathogenesis. Many of these loci are significantly underexpressed in tumors with *MYCN* amplification, which have particularly poor prognoses. Interestingly, we found that miRNA expression levels substantially change in a *MYCN*-amplified cell line following exposure to retinoic acid, a compound which is well known for causing reductions in *MYCN* expression and for inducing neuroblastoma cell lines to undergo neuronal differentiation. We also show that small interfering RNA inhibition of *MYCN* by itself causes similar alterations in the expression of miRNA loci. *In vitro* functional studies of one locus, miR-184, indicate that it plays a significant role in apoptosis. The association of experimentally induced alterations of miRNA expression in neuroblastoma cell lines with differentiation or apoptosis leads us to conclude that these loci play important roles in neuroblastoma pathogenesis. We further suggest that *MYCN* may mediate a tumorigenic effect, in part, through directly or indirectly regulating the expression of miRNAs that are involved with neural cell differentiation and/or apoptosis, warranting substantial further studies of miRNAs as potential therapeutic targets. [Cancer Res 2007;67(3):976–83]

Introduction

Neuroblastoma, one of the most common solid tumors in children, is derived from primitive cells of the sympathetic nervous system and is responsible for ~15% of all childhood cancer deaths (see ref. 1 for review). These tumors are particularly noted for extensive heterogeneity in clinical behavior, ranging from spontaneous regression to aggressive clinical course and death due to disease. This clinical heterogeneity is correlated, to some extent, with genetic abnormalities found in the tumors. At least three major genetic subtypes of the disease exist, including hyperdiploid/near triploid tumors that generally are associated with favorable outcomes, *MYCN*-amplified (MNA) tumors that have poor prognosis (2), and tumors characterized by hemizygous loss of chromosome 11q material, which are associated with poor survival (3, 4). Each of these genetic subtypes is also characterized by significantly different global gene expression profiles (5, 6). Additional chromosomal imbalances occur in each major unfavorable genetic subtype, some of which are nonrandomly distributed. For example, loss of distal chromosome 1p occurs preferentially in MNA tumors, whereas loss of chromosome 3p occurs primarily in the 11q− subtype (7–9). The most common chromosomal imbalance, gain of 17q, occurs at high frequency in all subtypes of advanced-stage neuroblastomas and has been associated with a poor clinical outcome in most studies (10–12). There are also many additional recurring large-scale chromosome imbalances that occur in neuroblastoma, which are not associated with prognosis but may nevertheless contribute to the disease.

The identification of genes that have been directly affected by chromosomal imbalances is complicated because large numbers of genes map to the regions of imbalance. The possibility that some tumor suppressor genes convey a tumorigenic effect through haploinsufficiency may be responsible for further complicating their identification. It is also possible that the dysregulation of multiple genes in the regions of imbalance is contributing to neuroblastoma pathogenesis (6). Intriguingly, it is also possible that some of the sequences with oncogenic effects in neuroblastoma are not conventional protein-coding gene sequences but rather nontranslated RNA sequences that have important regulatory functions. Many nontranslated RNA sequences, such as microRNAs (miRNA), map to the regions of genomic imbalance described above and may contribute to neuroblastoma pathogenesis.

miRNAs regulate gene expression at a posttranscriptional level by either inhibiting mRNAs from being translated or causing them to be degraded. They play major roles in the differentiation of neural (13) and other cell types, and the dysregulation of these sequences can have tumor suppressor or oncogenic activity in different forms of cancer. For example, two miRNAs (miR-15 and miR-16) mapping to chromosomal region 13q14 are frequently deleted and down-regulated in chronic lymphocytic leukemias and thus act as tumor suppressor genes (14). miRNAs acting in a dominant oncogenic manner are illustrated by another cluster of miRNAs (mir-17-92) on chromosome 13, which are coamplified and overexpressed in some lymphomas (15, 16). Some miRNAs, such as miR-21 on chromosome 17q, can have antiapoptotic effects in cancer cells (17, 18). Overall, the importance of miRNAs in cancer is illustrated by the fact that the expression profiles of a small set of miRNAs could classify multiple cancers more accurately than data from ~16,000 mRNAs (19). The finding that miRNAs are frequently located at fragile sites and genomic regions involved in cancers further implicates their involvement with malignant diseases (20).

Requests for reprints: Raymond L. Stallings, Children's Cancer Research Institute and Department of Pediatrics, The University of Texas Health Science Center at San Antonio, 8403 Floyd Curl Drive, Mail Code 7784, San Antonio, TX 78229-3900. Phone: 210-562-9028; Fax: 210-562-9014; E-mail: stallings@uthscsa.edu.

doi:10.1158/0008-5472.CAN-06-3667

Elucidating the role of miRNAs in cancer is clearly in its infancy, and to the best of our knowledge, there is presently only one published study on the role of miRNA dysregulation in pediatric cancer (21). It seems quite logical that miRNAs will be particularly important in pediatric cancer given their role in normal developmental processes and the fact that pediatric malignancies tend to involve perturbation of such pathways. Here, we have examined the differential expression of 157 miRNA loci, representing approximately one third of all known human miRNAs in three major genetic subtypes of neuroblastoma. We determine how miRNA expression profiles change following retinoic acid–induced differentiation of neuroblastoma cell lines, a compound used in the treatment of this cancer, which leads to reduced *MYCN* expression (22). Most significantly, we show that small interfering RNA (siRNA) inhibition of *MYCN* also alters the expression profiles of many miRNA loci. Transfection of one such locus, miR-184, into neuroblastoma cells was found to cause massive apoptosis and G_1 arrest. These results suggest that miRNAs play important roles in neuroblastoma pathogenesis.

Materials and Methods

Neuroblastoma tissue and cell lines. Primary neuroblastoma tumors were obtained from two sources: the Children's Oncology Group Tumor Bank (Philadelphia, PA) and a tumor bank at Our Lady's Hospital for Sick Children (Dublin, Ireland). The genetic abnormalities of the tumors were identified previously by metaphase comparative genomic hybridization (CGH), oligonucleotide array CGH, fluorescence *in situ* hybridization, or other techniques (5, 7, 23, 24). Histology from each specimen was reviewed and tumors were graded according to the International Neuroblastoma Pathology Classification system (Table 1). These tumors were selected to be representative of three genetic-clinical subsets (hyperdiploid, MNA, or 11q−) and therefore may not be broadly representative of unselected patients. The hyperdiploid tumors had a DNA index ranging from 1.25 to 1.54 and are characterized by whole chromosome gains and losses with few, if any, structural chromosome abnormalities. In particular, these tumors completely lack MNA, loss of 1p, 3p, and 11q, and gain of 17q material. All tumors were obtained at diagnosis before chemotherapy. The SK-N-AS and Kelly (N206) cell lines were obtained from the European Collection of Animal Cell Cultures (Porton Down, United Kingdom), whereas SK-N-BE was obtained from the American Type Culture Collection (Manassas, VA).

Stem-loop reverse transcription and Taqman real-time PCR. Total RNA was isolated with Trizol (Invitrogen, Carlsbad, CA) according to the instructions of the manufacturer. Stem-loop reverse transcription for mature miRNA was done as described previously (25). All reagents were obtained from Applied Biosystems (Foster City, CA). The Early Access kit, containing assays for 157 of the 474 miRNAs listed in the Sanger miRBase database, was used. Briefly, 5 ng of total RNA were reverse transcribed to cDNA with stem-loop primers and the Taqman MicroRNA Reverse Transcription kit. Quantitative real-time PCR was done by using an Applied Biosystems 7500 Real-time PCR System and a Taqman Universal PCR Master Mix. All PCR primers were from the Taqman MicroRNA Assays. Two different sequences, RNU19 and RNU66 [both are small RNAs encoded in the introns of *MATR3* (chr5:138642507-138642567) and *RPL5* (chr1:93,018,360-93,018,429; 1p22.1), respectively], were used for normalization. The comparative threshold cycle method was used to calculate the relative gene expression. PCR products were also analyzed on 3% agarose gels. *MYCN* expression was assessed by SYBR Green-based real-time PCR.

All-*trans*-retinoic acid treatment of neuroblastoma cells. The SK-N-BE cell line was selected for treatment with 5 μmol/L all-*trans*-retinoic acid (ATRA) because this cell line has previously been shown to be responsive to treatment (26). NB cells were seeded at 5×10^5 per 100-mm dish 24 h before treatment. ATRA (Sigma, St. Louis, MO) was continuously administered by replacing the medium every 24 h for 5 days. Cell morphology was monitored with a phase-contrast light microscope.

Table 1. Characteristics of primary tumors used in study

Tumor sample	Subgroup	INSS	Histopathology*
T-203	HYP	2b	Favorable
T-238	HYP	1	Favorable
T-269	HYP	2a	Favorable
T-1251	HYP	1	Favorable
T-1253	HYP	1	Favorable
T-1354	HYP	1	Favorable
T-296	HYP	2a	Unfavorable
T-347	HYP	1	Favorable
T-25	HYP	1	Favorable
T-1	HYP	2	Favorable
T-36	HYP	2a	Favorable
T-136	11q−	4	Unfavorable
T-283	11q−	4	Unfavorable
T-1100	11q−	4	Unfavorable
T-1194	11q−	4	Unfavorable
T-1220	11q−	4	Unfavorable
T-1352	11q−	4	Unfavorable
T-1359	11q−	4	Unfavorable
T-1012	11q−	4	Unfavorable
T-355	11q−	4	Favorable
T-1200	11q−	4	Favorable
T-31	11q−	4	Unfavorable
T-48	11q−	4	Unfavorable
T-433	MNA	4	Unfavorable
T-493	MNA	4	Unfavorable
T-1009	MNA	4	Unfavorable
T-1034	MNA	4	Unfavorable
T-1198	MNA	4	Unfavorable
T-1266	MNA	4	Unfavorable
T-1068	MNA	4	Unfavorable
T-1109	MNA	4	Unfavorable
T-14	MNA	4	Unfavorable
T-39	MNA	4	Unfavorable
T-53	MNA	2	Unfavorable
T-1406	MNA	2a	Unfavorable

Abbreviations: HYP, hyperdiploid; 11q−, loss of 11q; INSS, International Neuroblastoma Staging System.
*Histopathology classification using Shimada system based on patient age at diagnosis, degree of differentiation, and mitosis-karyorrhexis index.

Transfection of miR precursor molecules and *MYCN* siRNAs. miR precursor molecules (miR-184 and miR-30e) and negative control 1 precursor miRNAs were purchased from Ambion (Austin, TX). *MYCN* siRNA was purchased from Invitrogen (three different Stealth siRNA duplex oligoribonucleotides against *MYCN*). They were transfected into NB cells at final concentration of 10 nmol/L using LipofectAMINE RNAiMAX (Invitrogen) according to the manufacturer's instruction. Cells were harvested 24 h after transfection, and miR-184, miR-30e, and *MYCN* expression was analyzed by reverse transcription-PCR (RT-PCR) as described above.

Cell viability assay. A colorimetric assay based on the cleavage of the tetrazolium salt WST-8 by mitochondrial dehydrogenase in viable cells to a formazan dye was used following the manufacturer's instructions (Dojindo Molecular Technologies, Gaithersburg, MD). Briefly, NB cells were plated at 3×10^3 per well in 96-well plates with triplicate wells for each transfection. After the incubation period, 10 μL of cell counting reagent (WST-8) were added to each well, and incubation was continued for 2 h. Cell viability was

assessed by measuring the absorbance at 450 nm using a microtiter plate (ELISA) reader.

Apoptosis assays. The activation of executioner caspase-3 and caspase-7 in NB cells was determined using Caspase-Glo 3/7 Assay kit according to the manufacturer's instructions from Promega (Madison, WI). NB cells were plated in triplicate in 96-well plates and transfected as described above. Samples were read after 1 h of incubation with the caspase substrate on a SpectraMax Gemini M5 Microplate luminometer (Molecular Devices, Sunnyvale, CA). For cell cycle analysis, cells were stained with propidium iodide using a Cycletest Plus DNA Reagent kit (BD Biosciences, San Jose, CA) and analyzed with a FACSCalibur flow cytometer (BD Biosciences). The results were analyzed using ModFit LT software (BD Biosciences).

Statistical analysis. Kruskal-Wallis test (nonparametric ANOVA) with Student's *t* testing for comparison of two groups was used to analyze miRNA expression levels between the different genetic subgroups. A *P* value of <0.05 was considered statistically significant. A correction for multiple comparisons was also carried out using the Tukey-Kramer method. Statistical significance for caspase-3/caspase-7 activity was assessed using a Student's paired *t* test. Unsupervised hierarchical clustering was done using the centered correlation method in the program Cluster (27). Results were visualized with the Tree View program (27).

Results

Altered miRNA expression in different genetic subtypes of neuroblastoma tumors. miRNA expression was analyzed in primary neuroblastoma tumors by a stem-loop real-time PCR-based miRNA expression profiling method using the Taqman MicroRNA Assays Human Panel Early Access kit from Applied Biosystems, which includes 157 identified human miRNAs. Initially, we compared miRNA expression in a highly characterized set of 18 neuroblastoma, comprising low-stage hyperdiploid tumors with favorable histopathology ($n = 6$), high-stage 11q− tumors with unfavorable histopathology ($n = 6$), and high-stage MNA tumors with unfavorable histopathology ($n = 6$). For more accurate and reliable results, two internal control small RNAs, RNU19 and RNU66, were used to normalize the miRNA expression data. Very similar results were obtained using either RNU19 or RNU66 for normalization.

Thirty-seven of the 157 (~23.6%) miRNAs showed differential expression between the three categories of tumors, with *P* values derived from the nonparametric Wilcoxon/Kruskal-Wallis test being <0.05. To further validate our results, the 37 differentially expressed miRNAs were analyzed in another set of 17 neuroblastomas, comprising 5 hyperdiploid tumors, 6 11q− tumors, and 6 MNA tumors (Table 1). The expression of the miRNAs identified in the primary neuroblastoma tumor set was almost fully confirmed in this new set of samples. Data analysis of the combined 35 tumor samples indicated that 32 of the 37 miRNAs were significantly differentially expressed between the three categories of tumors using both RNU19 and RNU66 for normalization following correction for multiple testing using the Tukey-Kramer method (Fig. 1*A*; Table 2).

The binary comparisons of hyperdiploid low-stage tumors with favorable histology versus the 11q− or *MYCN* high-stage tumors with unfavorable histology showed differential expression of 6 and 23 miRNA sets, respectively (Table 2). The binary comparisons of MNA versus 11q− high-stage tumors with unfavorable histology showed differential expression of 12 miRNAs (Table 2). The difference in expression in these comparisons ranged from 1.6-fold to 12.3-fold, with 50% of expressional differences being >3-fold and 45% being >2-fold. Only three miRNAs are down-regulated in both MNA and 11q− tumors relative to the favorable tumors. Interestingly, miRNAs in MNA tumors were predominantly down-regulated ($n = 20$) as opposed to being up-regulated ($n = 3$; Fig. 1*A*; Table 2).

To characterize the molecular phenotype of human neuroblastoma, unsupervised two-way agglomerative hierarchical clustering analysis was done using the differentially expressed miRNAs across the entire sample set. We found no difference between analyzing results using either RNU19 or RNU66 for normalization (data not shown) and only consider the RNU66 data here. There were three main sample classes discovered in this analysis (Fig. 1*A*). One of the classes was composed exclusively of cases with genomic amplification of *MYCN*. The other two classes were heterogeneous with hyperdiploid and 11q− tumors, although clusters of 11q− or hyperdiploid tumors were observed. Interestingly, the same clustering patterns were observed based on mRNA expression profiling (5, 6).

Alteration of miRNA expression following retinoic acid–induced neuroblastoma cell differentiation. ATRA is known to arrest growth and induce differentiation in some NB cell lines. Hence, we evaluated the expression of these miRNAs in a MNA NB cell line (SK-N-BE) exposed to 5 μmol/L ATRA. ATRA treatment caused a marked morphologic differentiation characterized by the extension of neurites exceeding at least twice the length of the cell soma clearly detectable after 5 days (Fig. 2). Real-time PCR results revealed that 21 of 34 (61.8%) human miRNAs examined were altered >1.5-fold in SK-N-BE cells compared with the untreated control (Fig. 1*B*). The majority ($n = 17$) of these miRNAs were up-regulated in the ATRA-treated cells, whereas a small number ($n = 4$) were down-regulated. miR-184 showed the most dramatic alteration in expression, being up-regulated 9-fold after ATRA treatment. Two of the down-regulated loci, miR-181b and miR-92, were up-regulated in MNA tumors relative to the other tumor subtypes. Thirteen loci showed no significant change in expression.

SK-N-BE cells treated with ATRA for 5 days and then released from ATRA for 3 days had even higher levels of miR-184 (25×), indicating that the effects of ATRA treatment on miRNA expression continue for at least a short period after release.

Effects of siRNA inhibition of *MYCN* on miRNA expression in Kelly cells. Because *MYCN* is down-regulated in neuroblastoma cell lines exposed to retinoic acid (22), we have determined the effect of *MYCN* down-regulation on miRNA expression using siRNA inhibition of *MYCN*. Kelly cells (a MNA NB cell line also known as N206) were transfected with three different siRNAs (individually or in pools) targeting *MYCN*, and the level of silencing was quantified by real-time PCR. One siRNA, which showed maximal silencing effects, was selected for further experimental use. Quantitative real-time PCR analysis indicated at least a 60% reduction in *MYCN* mRNA levels relative to normal control cells transfected with a scrambled oligonucleotide (Fig. 3). Expression profiling of siRNA-transfected and normal control cells using a Taqman real-time PCR-based approach showed significant alterations in the expression of several miRNA loci (Fig. 1*B*). In most instances, the direction of expressional change was similar to that which was observed for ATRA. The two exceptions were miR-181b and miR-92, which decreased in ATRA-exposed cells and increased in the siRNA-transfected cells. Overall, however, this siRNA result was similar to the result obtained by ATRA, which also causes a reduction in *MYCN* expression, and suggests that MYCN either directly or indirectly regulates the expression of several miRNA loci that seem to be involved with NB cell differentiation. Inspection of

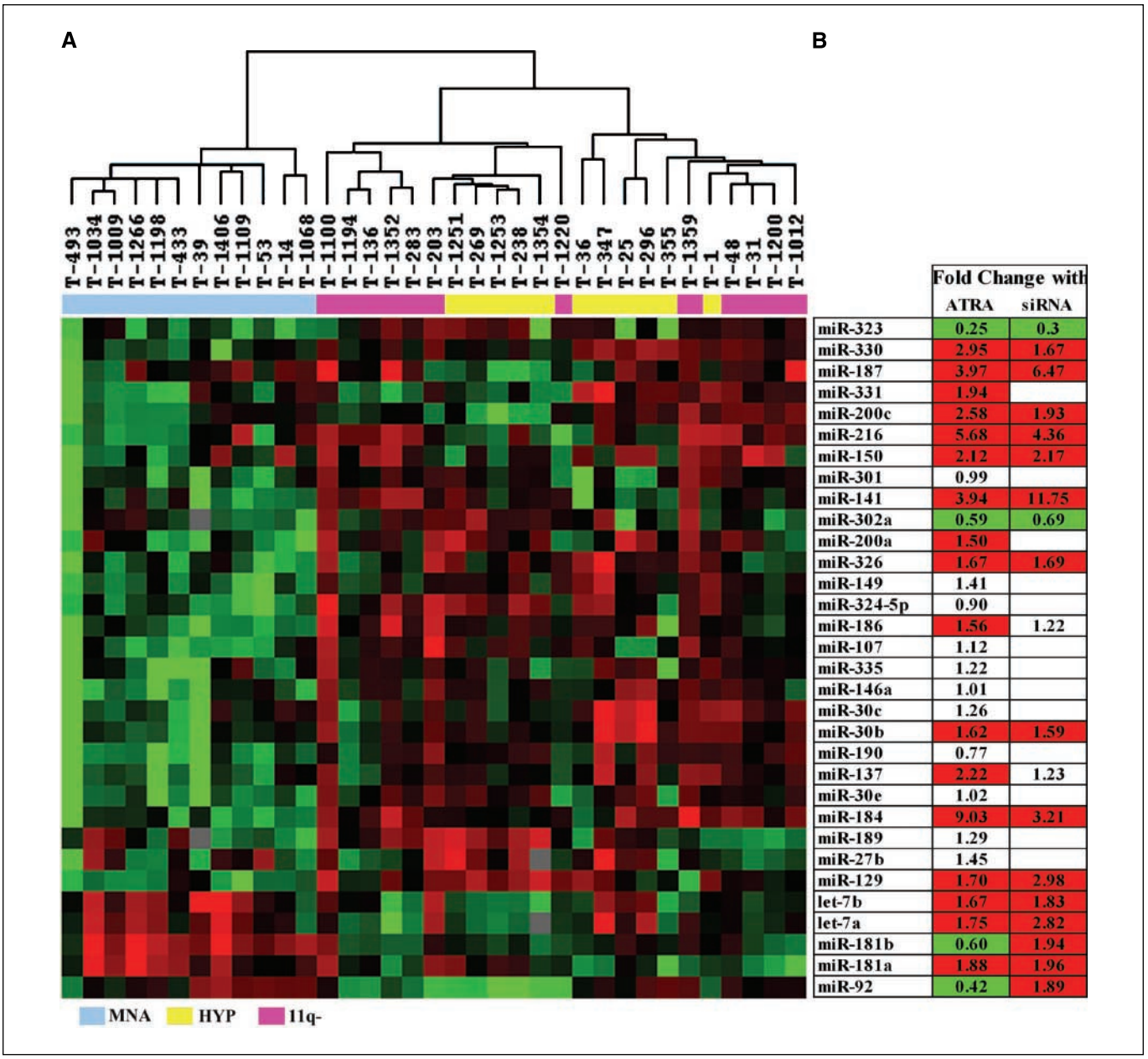

	Fold Change with ATRA	Fold Change with siRNA
miR-323	0.25	0.3
miR-330	2.95	1.67
miR-187	3.97	6.47
miR-331	1.94	
miR-200c	2.58	1.93
miR-216	5.68	4.36
miR-150	2.12	2.17
miR-301	0.99	
miR-141	3.94	11.75
miR-302a	0.59	0.69
miR-200a	1.50	
miR-326	1.67	1.69
miR-149	1.41	
miR-324-5p	0.90	
miR-186	1.56	1.22
miR-107	1.12	
miR-335	1.22	
miR-146a	1.01	
miR-30c	1.26	
miR-30b	1.62	1.59
miR-190	0.77	
miR-137	2.22	1.23
miR-30e	1.02	
miR-184	9.03	3.21
miR-189	1.29	
miR-27b	1.45	
miR-129	1.70	2.98
let-7b	1.67	1.83
let-7a	1.75	2.82
miR-181b	0.60	1.94
miR-181a	1.88	1.96
miR-92	0.42	1.89

Figure 1. Summary heat map of differentially expressed miRNA loci. *A,* heat map summarizing the patterns of expression for 32 miRNA loci that were differentially expressed in neuroblastoma subtypes. *Yellow,* low-stage hyperdiploid tumors with favorable histopathology; *pink,* high-stage 11q− tumors with unfavorable histopathology; *blue,* high-stage MNA tumors with unfavorable histopathology; *red,* high expression; *green,* low expression. MNA tumors form a distinct cluster characterized by low expression levels of many miRNA loci. The 11q− tumors formed two separate clusters, which could not always be perfectly distinguished from the low-stage hyperdiploid tumors. Interestingly, the same clustering patterns were observed based on mRNA expression profiling (5, 6). *B,* alterations in miRNA expression following ATRA exposure or siRNA inhibition of *MYCN*. The fold change in expression of miRNA loci following exposure of SK-N-BE cells to ATRA or Kelly cells to a *MYCN* siRNA was determined by the same quantitative real-time PCR-based approach used in the expression profiling of primary tumors. *Red,* increase in expression (>1.5-fold); *green,* decrease (>1.5-fold) relative to normal controls.

2,500-bp fragment of the miRNA promoters (−2,000 to +500) revealed the presence of putative MYCN-binding sites in the promoter region of many miRNAs (data available on request).

miR-184 overexpression induces neuroblastoma cell cycle arrest and apoptosis. miR-184 was significantly ($P < 0.01$) down-regulated in MNA tumors relative to expression in the other subtypes and was the most highly overexpressed miRNA locus (>9×) in SK-N-BE cells exposed to ATRA. To further evaluate the effects of overexpression of miR-184 in neuroblastoma, we transfected a MNA cell line (Kelly) and a *MYCN* single-copy cell line (SK-N-AS) with a double-stranded RNA (dsRNA) that mimics the miR-184 precursor. A similar approach has been used to study other miRNAs in mammalian cells (28). Elevated ectopic expression of miR-184 was confirmed by RT-PCR (Fig. 4*A*). Cell viability of Kelly and SK-N-AS cells assayed with WST-8 conversion [3-(4,5-dimethylthiazol-2-yl)-2,5-diphenyltetrazolium bromide (MTT) assay] was severely reduced with overexpression of miR-184 over time compared with the scrambled negative control (Fig. 4*B*). Cell

Table 2. Differential expression of miRNAs in neuroblastoma subtypes

miRNA	Chromosome map	MNA/hyperdiploid*	11q−/hyperdiploid*	MNA/11q−*
let-7a	22q13/9q22/11q24			2.4×
let-7b	22q13			3.99×
miR-27b	9q22.32	0.48×	0.36×	
miR-30b	8q24.22	0.44×		
miR-30c	1p34.2/6q13	0.44×		
miR-30e	1p34.2	0.24×		
miR-92	13q31.3/Xq26.2	3.64×		
miR-107	10q23.31	0.32×		
miR-129	7q32.1/11p11.2	0.08×		
miR-137	1p21.3	0.19×		
miR-141	12p13.31		2.09×	0.26×
miR-146a	5q33.3	0.25×		
miR-149	2q37.3	0.26×		
miR-150	19q13.33			0.34×
miR-181a	9q33.3	2.4×		3.75×
miR-181b	9q33.3/1q31.3	4.05×		8.85×
miR-184	15q25.1		2.2×	0.42×
miR-186	1q31.1	0.38×		
miR-187	18q12.2		2.92×	
miR-189	9q22.32	0.27×	0.39×	
miR-190	15q22.2	0.10×		
miR-200a	1p36.33	0.26×		
miR-200c	12p13.31			0.45×
miR-216	2p16.1			0.27×
miR-301	17q23.2			0.37×
miR-302a	4q25	0.39×		
miR-323	14q32.31	0.21×		0.27×
miR-324-5p	17p13.1	0.22×		
miR-326	11q13.4	0.35×	0.62×	
miR-330	19q13.32	0.29×		
miR-331	12q22	0.40×		0.63×
miR-335	7q32.2	0.45×		

*Fold difference in mean expression between the tumor subtypes being compared (i.e., MNA versus hyperdiploid, 11q− versus hyperdiploid, and MNA versus 11q−. *P* values obtained from one-way ANOVA ranged from <0.01 to <0.05, with 31 comparisons having *P* values of <0.01 and 10 comparisons having *P* values between 0.01 and <0.05. All comparisons were statistically significant when the Tukey-Kramer correction for multiple comparisons was applied.

viability reduction was noticed in both cell lines at 2 days after transfection, and dramatic loss of cell viability was apparent by day 5. To exclude the possibility of cell viability reduction due to the toxicity of the ectopically transfected dsRNA, we also tested overexpression of another miRNA (miR-30e) in the same NB cell lines. Although they have comparable miRNA expression levels, we did not find a cell viability change between transfected and negative control cells.

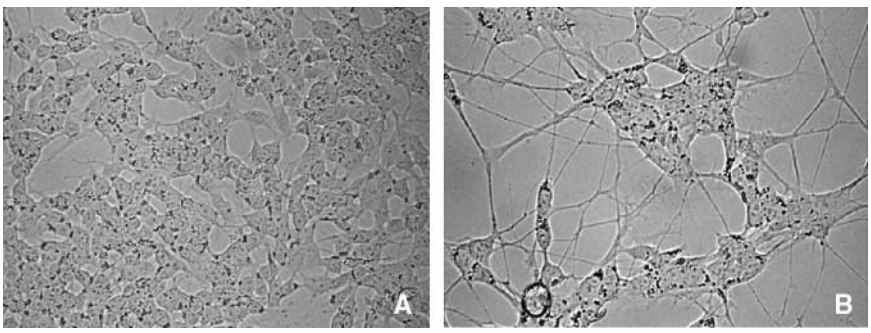

Figure 2. Induction of differentiation in neuroblastoma cells with ATRA. Untreated (*A*) and ATRA-treated (*B*; 5 μmol/L) SK-N-BE cells. The cells treated with ATRA had reduced proliferation and displayed neurite-like processes.

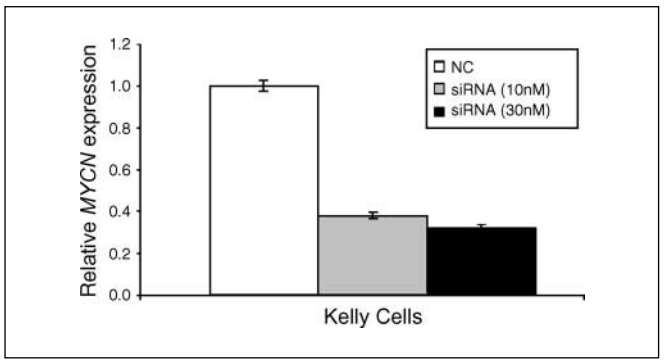

Figure 3. siRNA inhibition of *MYCN* mRNA. Quantitative RT-PCR analysis of *MYCN* expression in Kelly cells following transfections with a scrambled control oligonucleotide (*left column*) and commercially available *MYCN* siRNAs (*middle* and *right columns*). *Bars,* SD.

To determine the possible mechanism of antiproliferative activity of miR-184, we investigated its effect on cell cycle progression and apoptosis in the cell lines. Fluorescence-activated cell sorting (FACS) analysis revealed that miR-184 overexpression resulted in significantly higher number of cells in the G_1 phase compared with the scrambled negative control. As indicated in Fig. 4*C*, the effect of miR-184 on G_1 arrest in Kelly cells was largely at the expense of S phase cells with a minimal change in the G_2-M cell population. Cell number reduction was also associated with a marked increase in apoptosis (Fig. 4*C*). miR-184–induced apoptosis was further confirmed by examining caspase activity after transfection. Caspase-3 and caspase-7 enzymatic activities (key executioners of apoptosis) increased significantly (up to ~2-fold) by 72 h after transfection in cells treated with the miRNA precursor relative to the scrambled RNA–transfected control cells (Fig. 4*D*).

Discussion

MNA neuroblastomas are the most clinically aggressive subtype (2) so that the patterns of miRNA expression that are associated with this subtype are also correlated with a poor clinical outcome. MYCN can act as either a transcriptional repressor or activator depending on the locus in question (29), so it is tempting to speculate that overexpression of MYCN mediates a tumorigenic effect by down-regulating several miRNAs that are involved with neural cell differentiation or apoptosis.

Several findings reported in this paper are consistent with the concept that MYCN either directly or indirectly regulates the expression of several miRNAs that are involved with neuroblastoma pathogenesis. First, miRNAs have a nearly inverse pattern of expression in MNA tumors relative to other tumor subtypes, with the majority of miRNAs being dramatically underexpressed in the MNA tumor subtype. Second, ATRA, which causes the down-regulation of *MYCN* before neural differentiation (30), also leads to the up-regulation of several miRNA loci that are down-regulated in MNA tumors, along with the down-regulation of miRNAs that are up-regulated in the primary tumors. Although there are a couple of exceptions to the direction of change in miRNA expression, this seems to be a general pattern. Finally, and most significantly, direct siRNA-based inhibition of *MYCN* activity leads to very similar alterations in miRNA expression levels in MNA cell lines. Thus, it seems quite likely that MYCN either directly or indirectly regulates several miRNA genes, several of which have MYCN ebox-binding sites in close proximity (e.g., miR-184, miR-92, miR-129, and miR-187). In this regard, we note that another member of this gene family, MYC, has been shown to directly regulate a miRNA that regulates the E2F1 transcription factor (31).

The *MYCN* mRNA is a putative target of several of the miRNAs that are down-regulated in MNA tumors, including miR-107, miR-200c, and miR-302a, as determined by the TargetScan[1] and PicTar[2] target prediction algorithms. Although the targeting of the *MYCN* 3′-untranslated region by these miRNAs remains to be experimentally validated, if true, this explains why it is important for these miRNAs to be silenced in MNA tumors (i.e., expression of miRNAs that target *MYCN* would negate the effects of *MYCN* amplification).

For some neuroblastoma cell lines, exposure to ATRA causes apoptosis rather than the induction of differentiation. Although the factors that regulate whether a particular cell line will undergo differentiation versus apoptosis in response to ATRA are not completely defined, Niizuma et al. (32) recently reported that cell lines with lower levels of *BCL2* expression undergo apoptosis in response to ATRA, whereas those with higher levels of *BCL2* will differentiate. Our studies indicate that levels of miRNA expression also likely play a role in neuroblastoma cell apoptosis, given that overexpression of miR-184 causes both Kelly (*MYCN* amplified) and SK-N-AS (*MYCN* single copy) cell lines to undergo a caspase-mediated apoptosis. It is interesting to note that miR-184 has a more dramatic effect on Kelly cells, which have lower levels of endogenous miR-184 expression, similar to MNA tumors, than it does on SK-N-AS. Whether the overexpression or underexpression of a particular miRNA locus can also induce differentiation of neuroblastoma cell lines remains to be determined. In any event, a thorough understanding of the effects of retinoic acids on neuroblastoma cells is clearly important because 13-*cis*-retinoic acid improves patient survival when administered after intensive chemotherapy.

Many of the miRNAs (let-7a, miR-29b, miR-92, miR-107, miR-146, miR-128b, miR-181a, and miR-181b) that are differentially expressed in neuroblastoma subtypes have been noted to be involved in other forms of cancer (33–35) or with the control of cell proliferation (miR-187, miR-216, miR-301, and miR-150; ref. 36). The fact that ~38% of the miRNAs exhibiting differential expression in neuroblastoma subtypes are differentially expressed in other forms of cancer or have been shown to regulate cell proliferation is consistent with the concept that miRNA dysregulation plays an important role in the pathogenesis of these tumors. However, the effects of miRNAs could differ greatly in different cell types given that miRNAs mediate their effects through targeting mRNAs that are differentially expressed in tumors. The biological effects of miRNAs are further complicated by the fact that multiple mRNAs are usually targeted by a single miRNA.

The usefulness of miRNA expression profiling for classification of neuroblastoma tumor subtypes is also shown in this report. The profound down-regulation of many miRNAs in MNA tumors was the reason why such tumors formed a tight group following hierarchical cluster analysis. Overexpression of two miRNAs,

[1] http://www.targetscan.org
[2] http://pictar.bio.nyu.edu

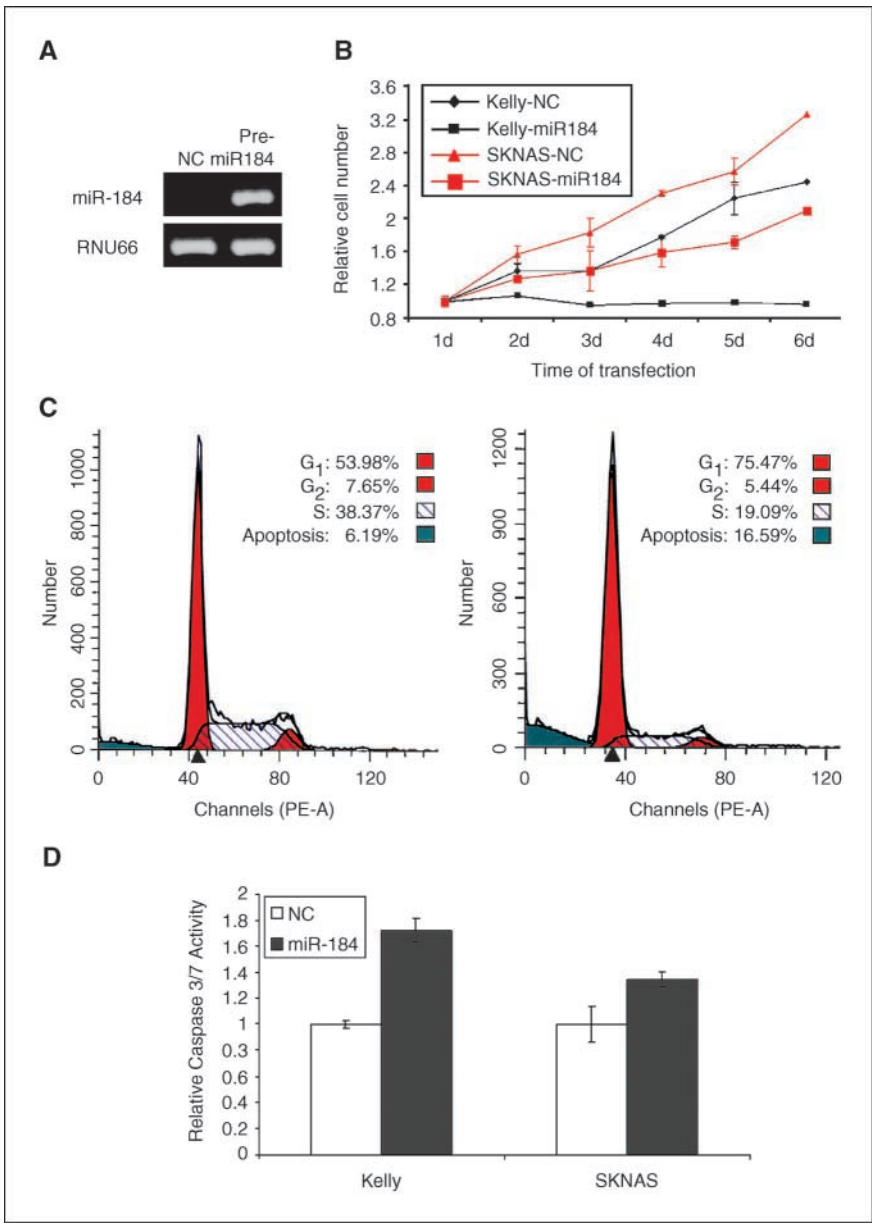

Figure 4. Analysis of neuroblastoma cell lines transfected with pre-miR-184. *A,* expression of miR-184 in Kelly cells transfected with a scrambled oligonucleotide [normal control (*NC*)] and with pre-miR-184 assessed by quantitative PCR. Virtually no miR-184 is present in Kelly cells. Expression of endogenous RNU66 (*bottom*) shows that equal amounts of PCR product were loaded onto the gel. *B,* analysis of cell viability using the MTT assay. *Y axis,* arbitrary units of measuring the accumulation of formazan dye in metabolically active cells; *X axis,* units of time in days. Measurements were taken at days 1 to 6 after transfection of Kelly (*black lines*) and SK-N-AS (*red lines*) with pre-miR-184 molecules or with scrambled control oligonucleotides. miR-184 slowed down cell proliferation in both cell lines but had a more dramatic effect in the MNA Kelly cell line. *C,* FACS analysis of Kelly cells transfected with scrambled oligonucleotide (*left*) or pre-miR-184 (*right*). The number of apoptotic cells increased in the Kelly cells overexpressing miR-184 (2.7-fold), and there was a substantial number of cells arrested at G_1 (54% versus 75.5%). *D,* analysis of caspase-3/caspase-7 activity in Kelly and SK-N-AS cells transfected with scrambled oligonucleotide (*white column*) or pre-miR-184 (*black column*). Both cell lines show an increase in apoptotic cells using the caspase-3/caspase-7 assay. Consistent with the MTT cell viability assay, the increase was more dramatic in the MNA Kelly cell line than in the *MYCN* single-copy cell line SK-N-AS. *Bars,* SD.

miR-216 and miR-150, was the distinguishing feature of 11q− tumors, which have a suboptimal clinical outcome not too different from MNA tumors (3). Although some discrimination between 11q− and low-stage hyperdiploid tumors was observed, these tumors could not be distinguished based on miRNA expression profiling with perfect accuracy. Interestingly, similar clustering patterns for hyperdiploid, 11q−, and MNA tumors were observed based on mRNA expression profiling (5, 6), which is not surprising given that mRNA levels can be affected by miRNAs (37, 38). Thus, clustering based on both mRNA and miRNA expression profiling suggests that hyperdiploid tumors and 11q− tumors are more similar genetically to each other than either is to MNA tumors in spite of the fact that 11q− tumors have unfavorable clinical outcomes. It seems likely that expression profiling with additional miRNA loci may lead to better classification in future studies, particularly because ~20% of the loci used in the current study were differentially expressed.

In summary, we have shown that exposure of neuroblastoma cells to ATRA causes profound alterations in miRNA expression levels and that direct siRNA inhibition of *MYCN* causes similar miRNA expressional alterations. Overexpression of miR-184, one of the most significantly altered miRNAs in the ATRA and siRNA experiments, causes massive apoptosis when introduced into Kelly or SK-N-AS cells, leading us to conclude that miRNAs have potential as therapeutic targets for the treatment of neuroblastoma and warrant substantial future studies.

Acknowledgments

Received 10/5/2006; revised 11/17/2006; accepted 11/27/2006.

The costs of publication of this article were defrayed in part by the payment of page charges. This article must therefore be hereby marked *advertisement* in accordance with 18 U.S.C. Section 1734 solely to indicate this fact.

We thank Dr. Sharon Murphy for her critical reading of the manuscript and insightful comments.

References

1. Brodeur GM. Neuroblastoma: biological insights into a clinical enigma. Nat Rev Cancer 2003;3:203–16.
2. Brodeur GM, Seeger RC, Schwab M, Varmus HE, Bishop JM. Amplification of N-myc in untreated human neuroblastomas correlates with advanced disease stage. Science 1984;224:1121–4.
3. Attiyeh EF, London WB, Mosse YP, et al. Chromosome 1p and 11q deletions and outcome in neuroblastoma. N Engl J Med 2005;353:2243–53.
4. Spitz R, Hero B, Ernestus K, Berthold F. Deletions in chromosome arms 3p and 11q are new prognostic markers in localized and 4s neuroblastoma. Clin Cancer Res 2003;9:52–8.
5. McArdle L, McDermott M, Purcell R, et al. Oligonucleotide microarray analysis of gene expression in neuroblastoma displaying loss of chromosome 11q. Carcinogenesis 2004;25:1599–609.
6. Wang Q, Diskin S, Rappaport E, et al. Integrative genomics identifies distinct molecular classes of neuroblastoma and shows that multiple genes are targeted by regional alterations in DNA copy number. Cancer Res 2006;66:6050–62.
7. Breen CJ, O'Meara A, McDermott M, Mullarkey M, Stallings RL. Coordinate deletion of chromosome 3p and 11q in neuroblastoma detected by comparative genomic hybridization. Cancer Genet Cytogenet 2000;120:44–9.
8. Plantaz D, Vandesompele J, Van Roy N, et al. Comparative genomic hybridization (CGH) analysis of stage 4 neuroblastoma reveals high frequency of 11q deletion in tumors lacking MYCN amplification. Int J Cancer 2001;91:680–6.
9. Vandesompele J, Van Roy N, Van Gele M, et al. Genetic heterogeneity of neuroblastoma studied by comparative genomic hybridization. Genes Chromosomes Cancer 1998;23:141–52.
10. Bown N, Lastowska M, Cotterill S, et al. 17q gain in neuroblastoma predicts adverse clinical outcome. U.K. Cancer Cytogenetics Group and the U.K. Children's Cancer Study Group. Med Pediatr Oncol 2001;36:14–9.
11. Brinkschmidt C, Christiansen H, Terpe HJ, et al. Distal chromosome 17 gains in neuroblastomas detected by comparative genomic hybridization (CGH) are associated with a poor clinical outcome. Med Pediatr Oncol 2001;36:11–3.
12. Vandesompele J, Baudis M, De Preter K, et al. Unequivocal delineation of clinicogenetic subgroups and development of a new model for improved outcome prediction in neuroblastoma. J Clin Oncol 2005;23:2280–99.
13. Miska EA, Alvarez-Saavedra E, Townsend M, et al. Microarray analysis of microRNA expression in the developing mammalian brain. Genome Biol 2004;5:R68.
14. Calin GA, Dumitru CD, Shimizu M, et al. Frequent deletions and down-regulation of micro-RNA genes miR15 and miR16 at 13q14 in chronic lymphocytic leukemia. Proc Natl Acad Sci U S A 2002;99:15524–9.
15. Calin GA, Liu CG, Sevignani C, et al. MicroRNA profiling reveals distinct signatures in B cell chronic lymphocytic leukemias. Proc Natl Acad Sci U S A 2004; 101:11755–60.
16. He L, Thomson JM, Hemann MT, et al. A microRNA polycistron as a potential human oncogene. Nature 2005;435:828–33.
17. Cimmino A, Calin GA, Fabbri M, et al. miR-15 and miR-16 induce apoptosis by targeting BCL2. Proc Natl Acad Sci U S A 2005;102:13944–9.
18. Chan JA, Krichevsky AM, Kosik KS. MicroRNA-21 is an antiapoptotic factor in human glioblastoma cells. Cancer Res 2005;65:6029–33.
19. Lu J, Getz G, Miska EA, et al. MicroRNA expression profiles classify human cancers. Nature 2005;435:834–8.
20. Calin GA, Sevignani C, Dumitru CD, et al. Human microRNA genes are frequently located at fragile sites and genomic regions involved in cancers. Proc Natl Acad Sci U S A 2004;101:2999–3004.
21. Kluiver J, Haralambieva E, de Jong D, et al. Lack of BIC and microRNA miR-155 expression in primary cases of Burkitt lymphoma. Genes Chromosomes Cancer 2006;45:147–53.
22. Thiele CJ. Patterns of regulation of nuclear proto-oncogenes MYCN and MYB in retinoic acid treated neuroblastoma cells. Prog Clin Biol Res 1991;366:151–6.
23. Stallings RL, Nair P, Maris JM, et al. High-resolution analysis of chromosomal breakpoints and genomic instability identifies PTPRD as a candidate tumor suppressor gene in neuroblastoma. Cancer Res 2006; 66:3673–80.
24. Stallings RL, Carty P, McArdle L, et al. Molecular cytogenetic analysis of recurrent unbalanced t(11;17) in neuroblastoma. Cancer Genet Cytogenet 2004;154:44–51.
25. Chen C, Ridzon DA, Broomer AJ, et al. Real-time quantification of microRNAs by stem-loop RT-PCR. Nucleic Acids Res 2005;33:e179.
26. Giannini G, Di Marcotullio L, Ristori E, et al. HMGI(Y) and HMGI-C genes are expressed in neuroblastoma cell lines and tumors and affect retinoic acid responsiveness. Cancer Res 1999;59:2484–92.
27. Eisen MB, Spellman PT, Brown PO, Botstein D. Cluster analysis and display of genome-wide expression patterns. Proc Natl Acad Sci U S A 1998;95:14863–8.
28. Garzon R, Pichiorri F, Palumbo T, et al. MicroRNA fingerprints during human megakaryocytopoiesis. Proc Natl Acad Sci U S A 2006;103:5078–83.
29. Valentijn LJ, Koppen A, van Asperen R, Root HA, Haneveld F, Versteeg R. Inhibition of a new differentiation pathway in neuroblastoma by copy number defects of N-myc, Cdc42, and nm23 genes. Cancer Res 2005;65:3136–45.
30. Thiele CJ, Reynolds CP, Israel MA. Decreased expression of N-myc precedes retinoic acid-induced morphological differentiation of human neuroblastoma. Nature 1985;313:404–6.
31. O'Donnell KA, Wentzel EA, Zeller KI, Dang CV, Mendell JT. c-Myc-regulated microRNAs modulate E2F1 expression. Nature 2005;435:839–43.
32. Niizuma H, Nakamura Y, Ozaki T, et al. Bcl-2 is a key regulator for the retinoic acid-induced apoptotic cell death in neuroblastoma. Oncogene 2006;25:5046–55.
33. Akao Y, Nakagawa Y, Naoe T. let-7 microRNA functions as a potential growth suppressor in human colon cancer cells. Biol Pharm Bull 2006;29:903–6.
34. Volinia S, Calin GA, Liu CG, et al. A microRNA expression signature of human solid tumors defines cancer gene targets. Proc Natl Acad Sci U S A 2006;103: 2257–61.
35. Ciafre SA, Galardi S, Mangiola A, et al. Extensive modulation of a set of microRNAs in primary glioblastoma. Biochem Biophys Res Commun 2005; 334:1351–8.
36. Cheng AM, Byrom MW, Shelton J, Ford LP. Antisense inhibition of human miRNAs and indications for an involvement of miRNA in cell growth and apoptosis. Nucleic Acids Res 2005;33:1290–7.
37. Lim LP, Lau NC, Garrett-Engele P, et al. Microarray analysis shows that some microRNAs down-regulate large numbers of target mRNAs. Nature 2005;433:769–73.
38. Wang X, Wang X. Systematic identification of microRNA functions by combining target prediction and expression profiling. Nucleic Acids Res 2006;34:1646–52.

Differential Patterns of MicroRNA Expression in Neuroblastoma Are Correlated with Prognosis, Differentiation, and Apoptosis

Yongxin Chen and Raymond L. Stallings

Cancer Res 2007;67:976-983.